Ultrasound-targeted Microbubble Destruction-mediated Gene Delivery Into Canine Livers

Misty L Noble[1], Christian S Kuhr[2], Scott S Graves[3], Keith R Loeb[3], Samuel S Sun[1], George W Keilman[4], Kyle P Morrison[4], Marla Paun[5], Rainer F Storb[3] and Carol H Miao[1,5,6]

[1]Center for Immunity and Immunotherapies, Seattle Children's Research Institute, Seattle, Washington, USA; [2]Benaroya Research Institute, Seattle, Washington, USA; [3]Fred Hutchinson Cancer Research Center, Seattle, Washington, USA; [4]Sonic Concepts Inc., Bothell, Washington, USA; [5]Applied Physics Laboratory, University of Washington, Seattle, Washington, USA; [6]Department of Pediatrics, University of Washington, Seattle, Washington, USA

Ultrasound (US) was applied to a targeted canine liver lobe simultaneously with injection of plasmid DNA (pDNA)/microbubble (MB) complexes into a portal vein (PV) segmental branch and occlusion of the inferior vena cava (IVC) to facilitate DNA uptake. By using a 1.1 MHz, 13 mm diameter transducer, a fivefold increase in luciferase activity was obtained at 3.3 MPa peak negative pressure (PNP) in the treated lobe. For more effective treatment of large tissue volumes in canines, a planar unfocused transducer with a large effective beam diameter (52 mm) was specifically constructed. Its apodized dual element configuration greatly reduced the near-field transaxial pressure variations, resulting in a remarkably uniform field of US exposure for the treated tissues. Together with a 15 kW capacity US amplifier, a 692-fold increase of gene expression was achieved at 2.7 MPa. Transaminase and histology analysis indicated minimal tissue damage. These experiments represent an important developmental step toward US-mediated gene delivery in large animals and clinics.

INTRODUCTION

The potential for therapeutic ultrasound (tUS) to augment minimally invasive nonviral gene transfer has long been recognized,[1–3] and a growing body of evidence indicates that significant enhancement of transgene expression can be achieved by using high-intensity acoustic energy. Effective US-mediated gene delivery relies on acoustic cavitation nucleated by exogenous microbubbles (MBs), or a method often described as US-targeted MB destruction (UTMD).[4–8] When cavitation nuclei are present, US exposures of suitable frequency and acoustic pressure can transiently increase the permeability of endogenous barriers such as capillary endothelium or cell membranes to otherwise impermeable materials (e.g., drugs or macromolecules). Many gene therapies have been attempted using direct intramuscular or intraparenchymal injection of gene vectors;[9,10] these vectors gain immediate access to the interstitial space, but must then traverse the plasma membrane of targeted cells. On the other hand, when gene transfer

vectors accompanied by MBs are administered intravascularly,[11,12] multiple barriers hinder entry of these vectors into cells. The first barrier encountered is the vascular endothelium (i.e., the hepatic sinusoids are rich in fenestrated endothelium). The next are other vascular anatomical features (e.g., the basement membrane and smooth muscle layer) and then the outer cell membrane of the cells, which one hopes to target. Finally, vector DNA needs to be transferred across the nuclear membrane to enter the nucleus for efficient gene expression. UTMD can potentially overcome some or all of these barriers, leading to significant enhancement of gene transfer efficiency. Our interest in this technology is to utilize nonviral gene therapy in conjunction with UTMD methods to increase the *in vivo* incorporation of plasmid DNA (pDNA) into liver cells with the aim of treating genetic diseases such as hemophilia.

We have demonstrated previously that US can significantly enhance gene transfection in mouse livers[13,14] when MBs and pDNA carrying a reporter luciferase gene, pGL4, were injected into the portal vein (PV) while US was applied to the liver lobes by using a simple, geometrically focused US transducer. However, this transducer was nearly ineffective when used in attempts to enhance gene transfer into rats. It became apparent that the effective treatment volume of the focused transducer was simply too small. A larger effective diameter transducer was designed for rat liver treatments and the delivery route was modified by injecting pGL4/MBs into a specific liver lobe through a PV branch (versus prior intraportal injection) with US exposure targeted to a specific liver lobe. With these modifications, we achieved a 100-fold increase in average luciferase expression in rats.[15] Further, it was found that a peak negative pressure (PNP) of about 2.7 MPa is required for effective gene transfection, with minimal liver tissue damage. Since liver volume increases rapidly with animal size, this was an important milestone toward translating this new technology to large animals.

To facilitate the eventual translation of these technologies into human application, many technical issues, such as surgical procedures, appropriate MB volumes, and US parameters and instrumentation require exploration in larger animal models. We chose dog as an appropriate large animal model because: (i) the size of the liver lobe of a small dog is similar to a portion of the human liver; (ii) the liver circulatory system is similar between dogs and human; and (iii)

Correspondence: Carol H Miao, Department of Pediatrics, Seattle Children's Research Institute, and University of Washington, 1900 Ninth Avenue, Seattle, Washington 98101, USA. E-mail: miao@u.washington.edu

dog disease models, such as canine hemophilia, are available. Here, we describe a new tUS system including a newly designed unfocused transducer for treating large tissue volumes in large animals. Further, we examine early parameterization experiments and treatment protocols to improve gene expression following US-mediated gene delivery into the dog liver.

RESULTS

Effect of transient IVC occlusion on MB retention in the liver

In a preliminary study (Dog 0), a wash-in/wash-out experiment was performed to determine appropriate volumes of delivered pGL4 and MBs to dog livers, as well as when and where these MBs distribute within the liver. Furthermore, occlusion strategies to improve pDNA/MB distribution and retention in liver lobes were also explored. In the first experiment, 300 µl of Definity MBs was injected into a patent PV with normal perfusion, followed by a saline line flush. MB distribution was immediately apparent in the liver lobes observed by diagnostic US imaging (**Figure 1a**). The MBs persisted in the liver for about 25 seconds, and by 75 seconds, most of the MBs were washed out *via* the venous

flow. Enhancement of MB contrast evaluated by pixel intensity (**Figure 1b**) as a function of time indicated that tUS treatment window was limited to within 25 seconds after injection. The transitory retention of MBs in the lobe suggested vascular occlusion would be required for longer MB retention. In the next procedure, hepatic outflow was interrupted by occlusion of the inferior vena cava (IVC) immediately before the MB bolus injection (300 µl of Definity) into the PV (**Figure 1c**). MBs were trapped in the liver and persisted for at least 2 minutes. A tUS transducer was then used to disrupt the MBs for 1 minute, resulting in the destruction of most MBs. Transient occlusion of IVC allowed the MBs to distribute diffusely throughout the liver lobes and persist for several minutes to allow tUS treatment. These wash-in/wash-out experiments set the condition/protocol for our subsequent studies on pDNA/MB delivery.

Development of tUS transducers for dog models

To treat large tissue volumes of canine liver, a dual-element planar unfocused transducer (H105) with a much larger effective beam diameter (52 mm) was designed and constructed. The apodized dual-element configuration was implemented to greatly reduce the
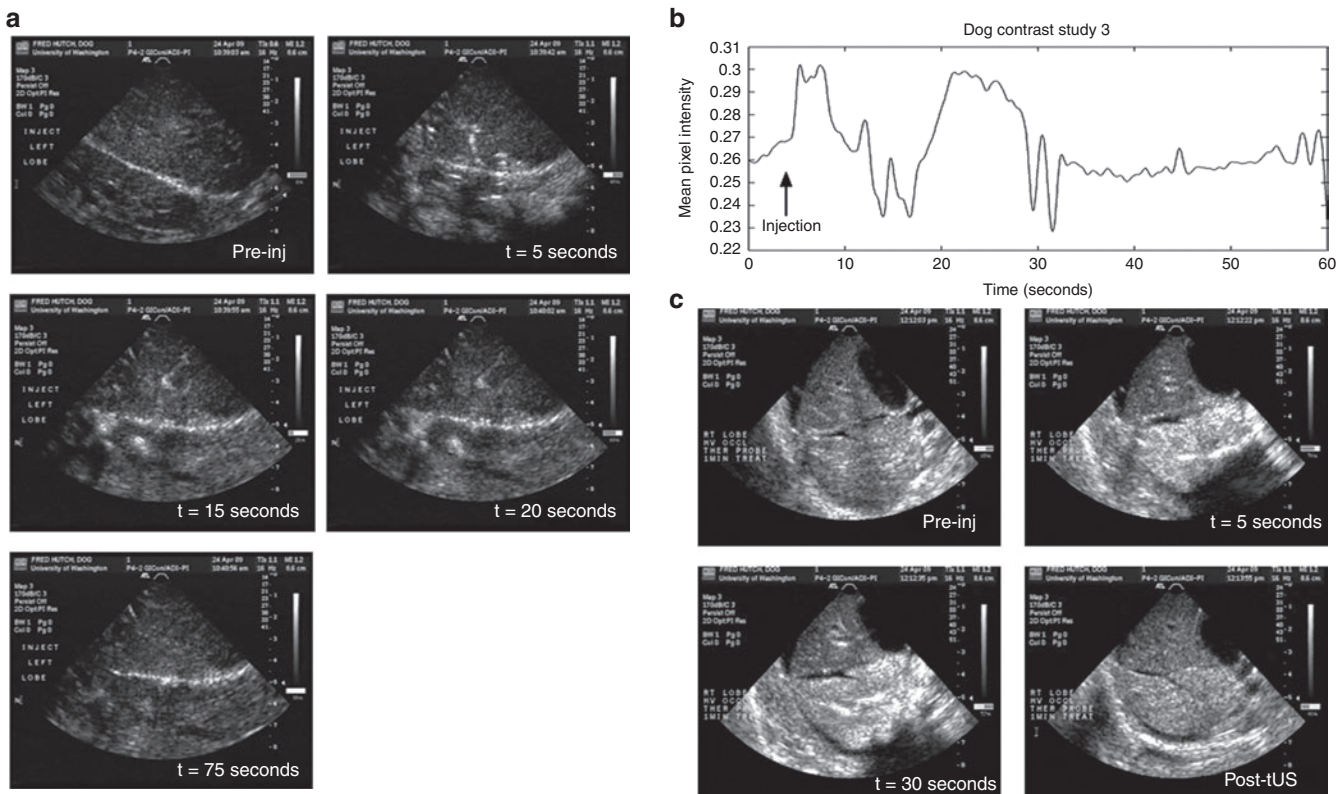

Figure 1 Ultrasound (US) imaging of microbubbles (MBs) injected into dog livers during wash-in and wash-out studies. Images were obtained using an HDI 5000 US imaging system (Philips Healthcare, Bothell, WA) equipped with a contrast-specific imaging package and a P4-2 transducer to illustrate the timing of MB flow dynamics. (**a**) US B-mode images of the dog liver were obtained before Definity MB injection (given as a 300 µl bolus into the portal vein (PV)), immediately after injection (5 seconds, first peak), 15 seconds post-injection (second peak), 20 seconds post-injection (third peak), and 75 seconds post-injection (return to background level). (**b**) A quantitative analysis of the persistence of MBs in the dog livers over time (from **a**) is shown as mean pixel intensity as a function of time. Upon injection of MBs, hyperechoic (or "bright") regions in the US image appear, and pixel intensities increase for a short time as the MBs are washed away with blood circulation. (**c**) Images obtained with venous occlusion. A bolus injection of Definity (300 µl) was instilled *via* segmental PV branch, whereas the IVC was clamped or occluded. Two liver lobes are visible in the diagnostic US images. MBs were trapped in the lower lobe immediately following injection with very few MBs entering the upper lobe, and these MBs persist in the lower lobe for at least 2 minutes. The liver was subsequently exposed to therapeutic US (tUS) for about 1 minute. The US image shows that most MBs are destroyed immediately following tUS exposure. Pre-inj, pre-injection.

near-field transaxial pressure variations and generate a uniform field for treating liver tissue. **Figure 2** shows pressure profiles of H105 transducer as point spread function calculations before (**Figure 2a**), and after (**Figure 2b**) apodization. The non-apodized configuration maintained the inner and outer elements of the H105 transducer at similar power levels, and the pressure delta over the radiating surface reached up to 4 dB (**Figure 2a**). In the apodized configuration (**Figure 2b**), the outer element was driven at 50% of the electrical amplitude of the inner element, which reduced the pressure delta to within 1.7 dB. This apodization strategy was validated by a pressure field map with small pressure variance over the transducer surface using a hydrophone at a distance of 1 mm from the transducer face (**Figure 2c**). The newly developed transducer was subsequently used for treating larger tissue volumes in dog experiments.

UTMD significantly enhanced gene expression in canine livers

In our previous rat studies, we investigated the effects of PNP on gene expression, and its associated liver tissue damage.

We found that a pressure amplitude of 2.7 MPa produced significant enhancement of luciferase expression with minimal damage in the rat liver.[15] We used these US conditions to commence our dog studies. The experimental conditions evaluated for UTMD-mediated gene transfer into dogs are summarized in **Table 1**. Two different US systems were used in delivering treatment with acoustic pressure amplitudes varying between 0 MPa (sham; transducer applied but not activated) and 3.3 MPa for 2–4 minutes of total tUS exposure time. The total volume of pGL4/MB solution injected also varied from 3.6 to 6.0 ml containing 1.5–3.0 ml Definity MBs in solution. Furthermore, we explored procedures to increase retention of pDNA/MB in the liver during tUS exposure to further enhance transgene expression, including: (i) different injection sites, (ii) different injection rates and durations, and (iii) different occlusion strategies. **Figure 3a** shows the luciferase expression for each dog in the study. Each symbol represents the luciferase activity measured in a small tissue section from treated or untreated control liver lobes, with the solid horizontal line representing average luciferase expression level. The liver lobes with
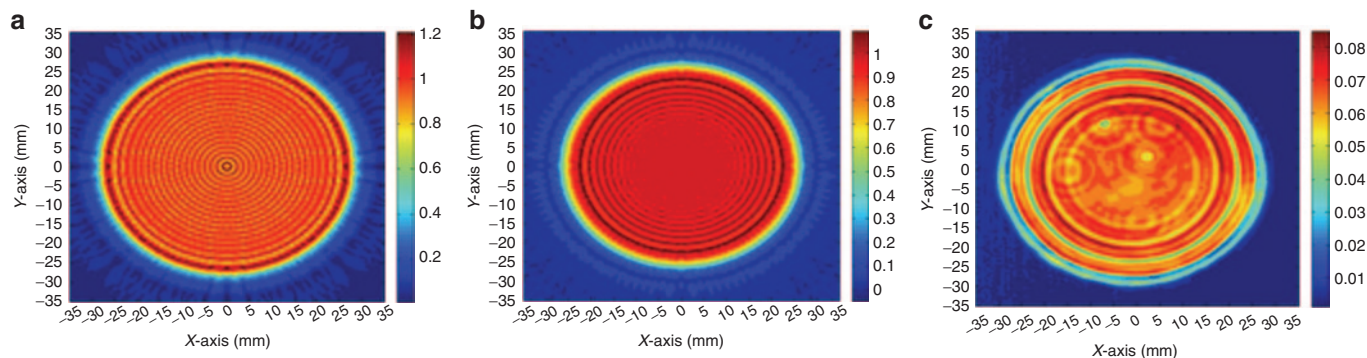

Figure 2 Pressure profiles of the apodized dual-element Sonic Concepts H105 transducer. Point spread function calculations of the dual-element H105 transducer is shown as pressure profiles (**a**) before and (**b**) after apodization. The pressure delta over the radiating surface can reach up to 4 dB in the non-apodized configuration (shown in **a**), but is greatly reduced to 1.7 dB after apodization by driving the outer element at 50% electrical amplitude of the inner element (shown in **b**). (**c**) A hydrophone was used to measure the actual pressure coming from the H105 transducer at a distance of 1 mm from its face. Relative pressure is encoded in color: warm colors indicate higher acoustic pressures; cool colors indicate lower pressures. Spatial scalars are 70-mm full range in each dimension, with an effective beam footprint of ~21 cm². Although there remain some transaxial inhomogeneities in the pressure field map, as indicated by modest annular structure, the near field of the transducer was remarkably uniform over most of the transducer face.

Table 1 Summary of experimental conditions used in ultrasound-assisted gene transfection studies in canines

Animal number	Definity injected volume (ml)	Total injected volume (ml)	Injection route	Injection time (seconds)	Outflow occlusion	Transducer used	Peak negative pressure (MPa)	Total US treatment time (minutes)
Sham	3.0	6.0	PV segment	60	IVC	H105	0	4.0
Dog 1	1.5	3.6	PV	Bolus	IVC	H158	2.7	2.0
Dog 2	1.5	3.6	PV segment	Bolus	None	H158	2.7	4.0
Dog 3	1.5	6.0	PV segment	60	IVC	H158	3.3	4.0
Dog 4	1.5	6.0	PV segment	60	IVC	H105	2.0	4.0
Dog 5	3.0	6.0	PV segment	60	IVC	H105	2.7	4.0
Dog 6	3.0	6.0	PV segment	60	IVC	H105	2.7	4.0
Dog 7	3.0	6.0	PV segment	60	IVC	H105	2.7	4.0
Dog 8	3.0	6.0	PV segment	60	IVC	H105	2.7	4.0

Abbreviations: IVC, inferior vena cava; PV, portal vein; US, ultrasound.
All dogs received 4 mg of pGL4, reporter luciferase gene. Microbubble used in all dogs is Definity.
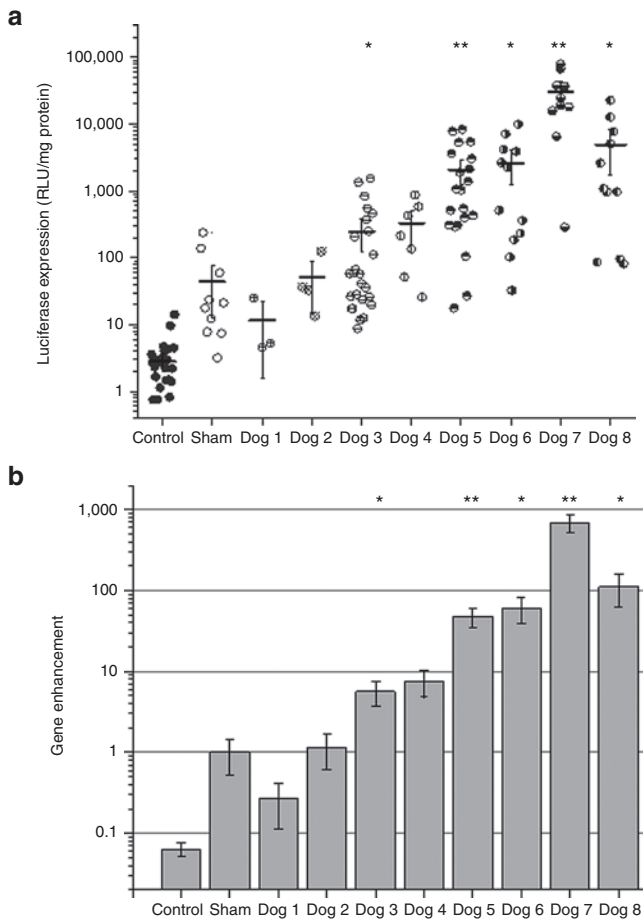
Figure 3 Luciferase gene expression following ultrasound-targeted microbubble destruction (UTMD)-mediated gene delivery into the dog livers. (a) Four milligrams of pGL4 plasmid and 1.5–3 ml of Definity MBs were injected *via* the portal vein (PV) or the segmental PV branch with simultaneous exposure of the target liver lobe to therapeutic US (tUS) (1.1 MHz frequency, 20 cycle pulses, 13.9–50 Hz pulse repetition frequency, and 2.0–3.3 MPa peak negative pressures (PNPs)) for 2–4 minutes using the small diameter transducer (H158) for dog experiments 1–3, or the large diameter transducer (H105) for dog experiments 4–8. A sham-treated dog received an equivalent pGL4/MB dose, but was not exposed to tUS (or 0 MPa PNP tUS exposure). Treated and untreated control lobes were harvested after 24 hours. Each lobe was sectioned, and the representative sections (shown as data points) were processed and assayed for luciferase activity. The average luciferase expression for each treated lobe is shown as horizontal lines, and the error bars indicate SEM (n = 3–15). *P < 0.05, **P < 0.005. **(b)** The average luciferase expression from each treated dog was normalized to the average luciferase expression of the sham-treated dog to determine the overall gene enhancement using modified surgical techniques and UTMD methods. Data showed stepwise improvement in gene enhancement with each dog experiment as occlusion strategies, proper MB injection site, and better tUS transducers and instrumentation were used. Error bars indicate SEM (n = 3–15). *P < 0.05, **P < 0.005. RLU, relative light unit.

neither US exposure nor direct injection of pGL4/MBs were used as negative controls, whereas the liver lobe from a dog treated with direct injection of pGL4/MBs but without US exposure was used as the sham control. US-assisted gene transfection for the first three dogs was performed using the single element, small diameter H158 transducer with the scanning rate of 5–10 mm/second

throughout the tUS treatment. In Dog 1, the pGL4/MB commixture was injected into the PV for distribution to the entire liver with IVC occlusion to retain pGL4/MBs longer. Luciferase expression levels were low (~10 relative light unit (RLU)/mg protein) probably due to low concentration of pGL4/MBs in the target lobe (left lateral lobe) at any specific time. In Dog 2, the pGL4/MB solution was injected into a segmental PV that allowed pDNA/MB to be concentrated into the targeted lobe. However, the IVC was not occluded, probably leading to rapid clearance of the pGL4/MB out of the liver. Luciferase expression was marginally improved relative to Dog 1 (~50 RLU/mg protein). In Dog 3, the pGL4/MB solution was injected into a PV segment after IVC occlusion with the acoustic pressure amplitude increased to 3.3 MPa. We obtained higher gene expression levels (~250 RLU/mg protein); however, the values were still not to the levels previously obtained in mouse and rat studies.[15]

In subsequent experiments, the specifically designed, unfocused H105 tUS transducer was used to treat larger tissue volumes per unit time. Similar power densities and pressure amplitudes as those we previously used with the smaller H158 tUS transducer in the rat studies were produced with the newly assembled US system consisting of a powerful Ritec pulse generator/power amplifier system (**Table 1**). In Dog 4, luciferase expression improved (~330 RLU/mg protein) using 2 MPa PNP US with transient IVC occlusion and PV segment injection. Increasing the PNP to 2.7 MPa resulted in additional improvement of gene transfection (~600 RLU/mg protein, data not shown). Subsequently in Dog 5, a significant increase in luciferase expression (~2,100 RLU/mg protein) was observed when the targeted liver lobe was exposed to 2.7 MPa PNP and the MB dose was increased from 1.5 to 3.0 ml Definity. This result was replicated in Dog 6, 7, and 8 experiments (average ranging from 2,600 to 30,500 RLU/mg protein) using the same treatment conditions.

The average luciferase gene expression from each dog was normalized to the average luciferase sham-treated values and plotted in **Figure 3b**. A steady improvement in luciferase gene enhancement was observed with each successive experiment. Average luciferase expression has improved by 692-fold in Dog 7, and up to 1,800-fold enhancement in some tissue sections, compared with the sham-treated dog.

Minor tissue damage revealed in histological and transaminase analysis

Liver biopsies were performed 24 hours following surgery to examine any potential hepatic injury. Representative hematoxylin and eosin-stained slides of sham-treated and US-treated dogs are shown in **Figure 4**. Sections were taken from central subcapsular areas maximally exposed to tUS, as well as, from control lobes without US exposure. Control and treated lobe sections of both sham-treated (**Figure 4a,b**) and US-treated (**Figure 4c–h**) dogs had intact hepatic architecture with mild edema, sinusoidal, and vascular congestion that was attributed to the extrahepatic vascular outflow obstruction used in the procedure. In the majority of dogs, the only histologic change associated with US treatment were minor focal subcapsular hemorrhage and acute inflammation attributed to manipulation with the tUS transducer and application of the US coupling gel. Only Dog 7, which produced
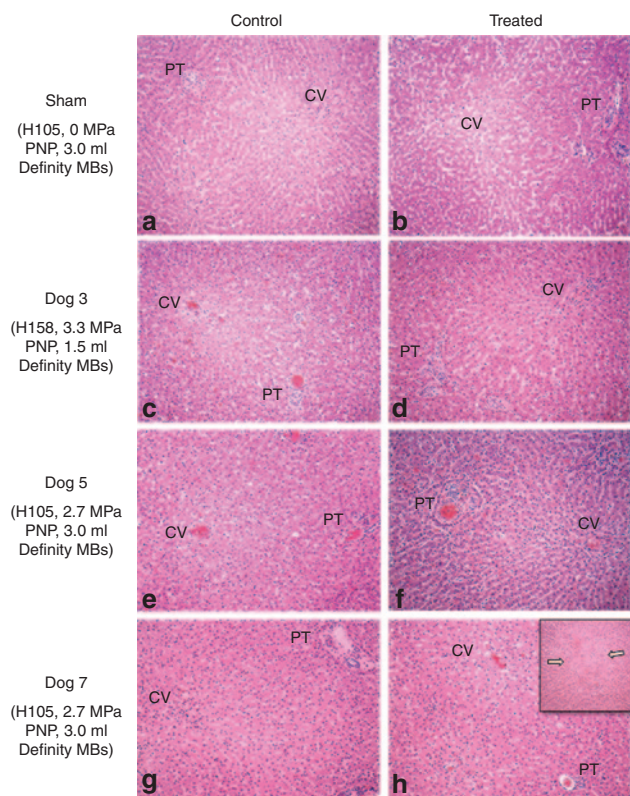
Figure 4 Histological analysis of treated and control livers showed minimal damage. Representative hematoxylin and eosin-stained images showing the portal tract (PT) and central vein (CV) from treated dogs are shown. Control and treated liver lobes from various dogs are shown on the left and right columns, respectively. (**a**,**b**) Analysis of the sham control and treated livers, respectively, reveals dilatation of the sinusoids around the CV. No significant difference between the livers is found. In Dog 3, (**c**) the treated lobe does not reveal any focal necrosis that can be attributed to the 3.3 MPa peak negative pressure (PNP) ultrasound treatment (using H158), and (**d**) remains comparable to its control lobe. (**e**,**f**) A slight increase in inflammatory response (increased leukocyte infiltration) is observed in Dog 5, which was injected with 3 ml Definity microbubbles (MBs) and treated using H105 transducer at 2.7 MPa PNP. (**g**,**h**) The average luciferase expression in Dog 7 was the highest (to date), and a focus of mild tissue damage is observed in the treated lobe (as shown in **h**) using H105 transducer at 2.7 MPa. Evident architectural disruption in the CV area is shown (inset), as well as increased leukocyte infiltration and small areas of focal necrosis. All images were originally obtained at ×10 magnification.

the highest level of luciferase expression, showed a rare focus of hepatic architectural disruption and hemorrhage in a pericentral venous pattern with lymphocytic inflammation, rare hepatocyte sloughing, and endothelial disruption associated with the distended central veins (**Figure 4h**, inset). No significant histologic differences between the US-treated and control liver biopsies were observed in the other dogs. In general, all of the histologic damage was minimal; and based on our previous studies would be quickly repaired without long-term sequelae.

Alanine aminotransaminase (ALT) (**Figure 5a**) and aspartate aminotransaminase (AST) (**Figure 5b**) liver enzyme levels were examined to determine possible US-induced impact on liver damage. No difference in ALT and AST levels was obtained between sham-treated and normal dogs. Dog 3, which was exposed to a higher acoustic PNP (3.3 MPa) had more significantly elevated
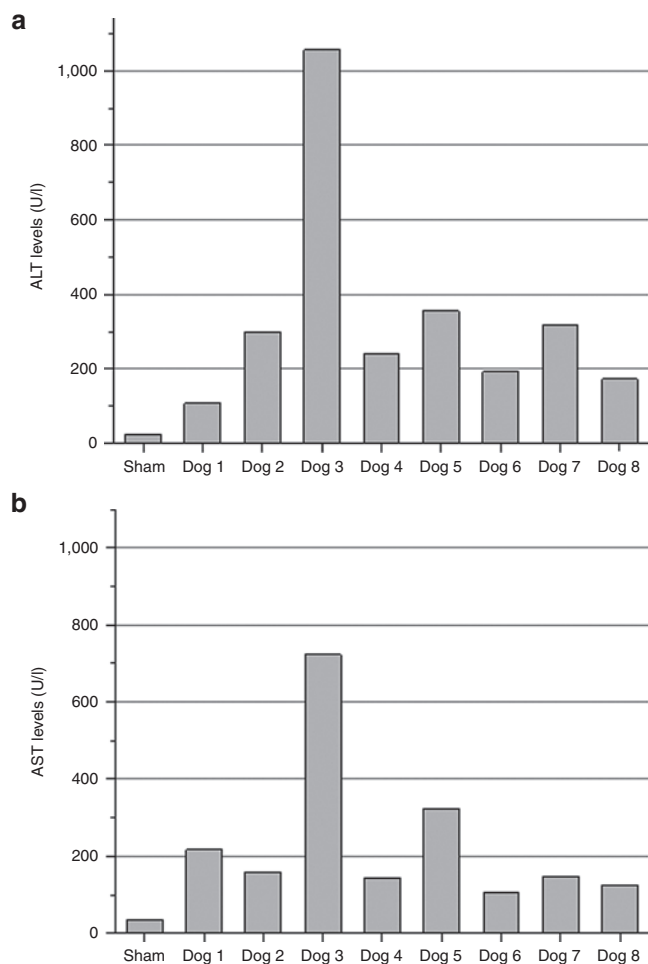
transaminase levels. All other US-treated dogs showed a very mild elevation of transaminase levels 24 hours after treatment, indicating minor liver damages. These results are consistent with the histological analysis of the liver tissue.

DISCUSSION

The main goal of this study was to scale up plasmid-based delivery of transgenes to the liver of rodents to large animals. The experimental dogs used in this study weighed between 10 and 20 kg, and their livers were about 100- to 500-fold larger than mouse or rat livers. Linear scaling of reagent concentrations and volumes is not practical. Accordingly, parameterization experiments involving injection volumes and rates, surgical procedures, MB concentrations, and US exposure and instrumentation were initiated in this study. First, wash-in/wash-out studies with US contrast agent MBs injected into the PV or the PV segmental branches showed that pDNA/MBs entered and evacuated the liver rapidly *via* normal blood flow, leaving a small treatment window (~25 seconds) for tUS application. To improve retention of pDNA/MBs in the liver, outflow from the liver during injection of the pGL4/MBs solution was impeded by temporarily clamping the IVC. The MBs were distributed robustly and evenly into a specific liver lobe, and retained for several minutes. Using this procedure, the majority of the MBs were destroyed by exposing the liver to tUS at sufficient acoustic pressure amplitude, achieving desired bioeffect—*i.e.*, permeabilization of the tissues and cells to plasmids.

By injecting pDNA/MB solution into the PV segmental branch with IVC occlusion, a small hydrodynamic component may have contributed to the increase in transgene expression (see sham-treated dog data in **Figure 3**), but this component was one to several orders of magnitude less than that attributable to US treatment. Hydrodynamic gene transfection procedures usually involve instillation of large volumes of fluids (about 10% of body weight) injected in a very short amount of time. In a study in pigs, a total volume of 600 ml was injected in 15 seconds to create a 75 mmHg pressure increase with IVC occlusion.[16] We injected total volume of 6 ml at a much slower rate of 1 ml/10 seconds into a specific liver lobe, which was treated directly with tUS. There is very minimal hydrodynamic effect by our procedure, and most of the gene transfection should be attributed to UTMD.

Our previous studies showed that 2.7 MPa PNP generated by the single element, small diameter H158 transducer is sufficient to produce the desired transfection effect with minimal tissue damage in rats.[15] However, the H158 transducer was inefficient in delivering luciferase plasmid into dog livers. It was imperative to develop a new tUS transducer H105 with a bigger acoustic footprint to more quickly and uniformly treat the canine liver with large tissue volumes. Compared with the 13-mm diameter H158 transducer, which was driven by a 1-kW capacity power generator, the H105 transducer is 52 mm in diameter with ~16-fold larger surface area. To generate the similar acoustic conditions and power density as H158, the H105 transducer required a power generator capable of delivering up to 15 kW. Application of this large, planar, apodized H105 transducer produced far superior transgene expression than the smaller H158 transducer at 2.7 MPa, indicating the importance of being able to acoustically treat large tissue volumes during the relatively short time when MBs and plasmids remain

Figure 5 Evaluation of serum liver transaminase levels (alanine aminotransaminase (ALT) and aspartate aminotransaminase (AST)) in treated and control dogs. Blood was collected from all experimental and sham-treated dogs 24 hours post-surgery. A complete blood count and chemistry panel was performed. Most analytes were found to be within normal limits. Liver enzymes, (**a**) ALT and (**b**) AST, were found to be slightly elevated in ultrasound (US)-treated animals. Dog 3 showed higher ALT and AST levels, which could be due to the higher US pressures used in treatment.

in the liver. Similarly to the rat experiments, we targeted a specific liver lobe by directed delivery of MBs and plasmids *via* the segmental PV. This modification resulted in lower tissue volumes for treatment and higher local concentrations of plasmids and MBs in the treated lobe. We also tested a limited number of MB dose regimens and found that higher MB doses produced significantly superior gene expression. Variability of gene expression within a single-treated liver lobe was observed, probably due in part to the disproportionate US exposure of various areas. Middle sections of the liver with easy access to the tUS transducer usually generated higher gene expression, whereas the peripheral portions with more difficult access generated lower luciferase expression. The variability could also be related to vascularity, as central regions of the lobe are better supplied with relatively large vessels.

tUS has been used to obtain a wide range of bioeffects in various medical applications.[17–19] In our case, it is used to cavitate exogenous nuclei, *i.e.,* MBs that could transiently permeabilize the vascular

endothelium and cell membranes to allow entry of plasmids into cells. The acoustic conditions were chosen to reduce any damages or harmful side effects on the treated tissue or the surrounding organs. Very short US pulses (20 cycles) at low frequency (1.1 MHz) and high pressure amplitudes (2.7 MPa) are inductive towards creation of cavitation conditions for MBs present in the region. The resulting low duty cycle (0.091%) should have prevented any heating effects. Cavitation and other mechanical bioeffects can lead to apoptosis[20,21] and severe hemorrhaging due to breakdown of capillaries from mechanical shear stresses of MB dynamics.[22,23] In our study except for Dog 3, very mild elevation of the ALT and AST levels was observed in US-treated dogs, indicating minimal hepatic injury associated with the procedure. Higher elevation of transaminase levels observed in Dog 3 was attributed to higher PNP (3.3 MPa) at which more violent MB cavitation occurs, and thus generating more tissue damage. Although our sham-treated dog showed normal levels of ALT and AST, ischemic conditions within the liver created during IVC occlusion could have also contributed to elevation of these liver enzymes.[24,25] There were no gross hepatic changes detected during necropsy. These acute vascular events coupled with US-induced permeabilization led to some minor liver tissue trauma. Assessment of liver injury by histology revealed no significant tissue damage, *i.e.,* apoptosis or necrosis, in random-treated tissue sections. There were some areas of sinusoidal dilatation that was most likely due to the IVC occlusion and pGL4/MB instillation, as these features were also observed in the sham-treated and control lobes.[26–28] Overall, these results are consistent with what was observed in our previous rat studies; viz., that the UTMD treatments did not generate extensive or irreparable liver damage.[15] We have no long-term survival data for dogs and thus cannot say how rapidly the treated dog livers recover from treatment, but in our rat studies, the transient minor damage was repaired quickly within a few days.

Unlike viral gene delivery, there are minimal immunologic or toxicity challenges in gene transfection with UTMD. Our previous experiments in mice (C.H. Miao, S. Song and M.L. Noble, unpublished data) showed that *in vivo* UTMD methods generated much better transfection results compared with synthetic gene delivery vehicles using commercially available products, such as Lipofectamine and polyethyleneimine. Compared with other physical methods of gene delivery, UTMD can significantly enhance gene transfer efficiency with minimal tissue damage. In addition, MBs and tUS transducers can be designed and engineered to further enhance gene transfection. Furthermore, tUS transducers can be constructed such that the US focus is farther away from the face of the transducer, which will enable us to treat tissue transcutaneously.

In conclusions, our data demonstrated that: (i) increasing the retention time of MBs and plasmids in tissue during tUS treatment enhanced gene transfer efficiency, (ii) the larger unfocused tUS transducer was much more efficient in treating large tissue volumes of canine livers than the smaller transducer used in small animals; (iii) gene delivery efficiency was improved by increasing MB concentrations; and (iv) gene expression levels were significantly enhanced by using the new transducer with a larger footprint at 2.7 MPa PNP with minimal tissue damage in dogs. Our results demonstrate that large tissue volumes can be acoustically treated effectively with suitable transducer technology, and successful UTMD-mediated gene therapy technology has been developed in large animal models and will be applicable to clinical treatment.

MATERIALS AND METHODS

Animal use protocol. All procedures were performed according to the guidelines for animal care of both the National Institutes of Health and Seattle Children's Research Institute, with protocol approval of Institutional Animal Care and Use Committees of both Seattle Children's Research Institute and Fred Hutchinson Cancer Research Center. A total of eight dogs were enrolled in the study. The dog experiments were performed in the canine facility of Fred Hutchinson Cancer Research Center.

Plasmids and MBs. A luciferase reporter plasmid with an SV40 promoter, pGL4.13 (luc2/SV40) (Promega, Madison, WI) was produced by GenScript (Piscataway, NJ) according to the standard techniques. In each of the gene transfer studies, 4 mg of pGL4 was mixed with 1.5–3 ml of Definity US contrast agent MBs (Lantheus Medical Imaging, North Billerica, MA) and diluted with phosphate-buffered saline for a total volume of up to 6 ml per injection. Definity MBs, which are generally used for enhancing contrast in cardiac US imaging, were generated by shaking the vial for 45 seconds with a Vialmix agitator (Lantheus Medical Imaging, North Billerica, MA) immediately before preparing the pGL4/MB commixture. Definity MBs have a phospholipid shell that entraps a denser octafluoropropane gas, and are usually between 1.1 and 3.3 μm in diameter. The average MB concentration of Definity is ~6.2×10^9 MBs/ml, with a maximum concentration of up to 1×10^{10} MBs/ml. It is estimated that there are approximately between 10 and 20 billion MBs in each injection.

tUS systems. Two tUS systems were used in this study. The first tUS system was previously described by Song *et al.*[15] In this system, a single-element transducer (H158; Sonic Concepts, Bothell, WA) with a fundamental frequency of 1.1 MHz and an effective beam diameter, *i.e.,* full width, half-maximum, of 13 mm was used. This corresponds to a treatment area of about 1.3 cm². The system was driven by a combination pulse generator and radio-frequency amplifier (RFG-1000; JJ&A Instruments, Duvall, WA) that is capable of producing up to 1,000 W of electrical power with a 50 Ω load. US was delivered by direct application of the transducer to the liver; *i.e.,* the exposures were in the near field of the transducer, the pressure profiles of which had the expected transaxial peaks and valleys, and axial peaks and nulls. Spatial average PNPs ranged from 2.7 to 3.3 MPa. Pulse repetition frequencies ranged from 12.5 to 13.9 Hz for 2–4 minutes of total tUS exposure.

The second tUS system featured a much larger, dual-element transducer (H105; Sonic Concepts). With a fundamental resonance frequency of 1.1 MHz, this H105 transducer has an effective beam diameter of ~52 mm, which corresponds to a treatment area of about 21 cm². This transducer was better scaled to the size of the canine liver, and was designed to produce more uniform near-field acoustic exposures when applied directly to the liver. A custom software interface (Sonic Concepts) was used to control the combination pulse generator and radio-frequency power amplifier (RPR-4000-HP Pulser/Receiver; Ritec, Warwick, RI) that has a maximum electrical power output of 15 kW. US was delivered by this transducer at spatial average PNPs of 0 (sham) to 2.7 MPa (experimental animals) using 20 cycle pulses, 50 Hz pulse repetition frequency, and for 4 minutes of total tUS exposure.

Canine surgery. After induction of general anesthesia, each dog was placed in supine position. The abdomen was shaved, prepped, and draped in a sterile fashion. A midline laparotomy was performed, and a balfour retractor was used to further enhance exposure of the liver. The right and left hepatic lobes were mobilized by incising the triangular ligaments, and the vasculature of three lobes of the liver was isolated for infusion. Two infusions were performed into two liver lobes while diagnostic US monitoring was conducted. PV segmental branches were cannulated with an 18-G angiocath, and the IVC was clamped to occlude outflow before injection of the pGL4/MB solution. tUS was applied shortly afterward with simultaneous instillation of the pGL4/MB commixture. Contrast visualization was enhanced during the dwell time, and wash-out followed release of the

outflow occlusion. The cannulation sites were repaired with 5-0 Prolene figure-of-eight sutures. At the conclusion of the procedure, warm saline was placed in the peritoneal cavity for resuscitation and supplemental warming. The incision was sutured, and the skin was closed with surgical staples. Dogs were given postoperative local (lidocaine) and systemic (buprenorphine) analgesia. After recovery from anesthesia, they were monitored overnight. Twenty-four hours after the procedure, dogs were euthanized, and blood and tissue samples were collected for luciferase and transaminase assays, and for histological evaluation.

MB distribution visualization using US imaging. In each experiment, the target liver lobe was visualized using either a CL10-5 (central frequency (F_0) = 7.5 MHz, and mechanical index = 0.3) or a P4-2 (F_0 = 3 MHz and mechanical index = 1.3) imaging transducer connected to an HDI 5000 imaging system (Philips, Bothell, WA) to detect the presence of MBs and their distribution in the target area before and after tUS treatment. The HDI 5000 system used is equipped with a contrast-specific imaging package that allowed for pulse inversion imaging to increase sensitivity to MBs. The grayscale B-mode images were digitized, and imported into MATLAB (The Mathworks, Natick, MA) for analysis. A set of pixels circumscribing the liver were manually selected before MB injection, and the average pixel intensity within the region was calculated. A two-dimensional cross-correlation speckle tracking algorithm was implemented to track the movement of each of the manually selected pixels, and the mean intensity within the new motion-compensated circumscribed region for each frame was calculated.

Gene expression evaluation by luciferase assay. To evaluate luciferase gene expression, US-treated liver lobes were resected following sacrifice of the animal 24 hours after procedure. A control lobe, which was not directly injected with the pGL4/MB solution and was not exposed to tUS, was also collected for comparison. Treated and control lobes were further sectioned into smaller pieces, and some of these samples were used in assessing gene transfer *via* luciferase assay, and others were fixed for histological examination (described later). Tissue samples for luciferase assay were homogenized in reporter lysis buffer (1X) (Promega) at a ratio of 3 ml/g of tissue. The cell lysate was exposed to three freeze-thaw cycles to ensure complete release of the luciferase protein. The homogenates were then vortexed and centrifuged at 18,000*g*, and the supernatant was then transferred and stored at −80 °C until measurement. Luciferase assay was performed with a commercially available kit (Luciferase Assay System, cat. no. E1500; Promega), and the light produced by the oxidation of luciferin was measured by a luminometer (Victor 3; Perkin-Elmer, Wellesley, MA). The luciferase activity was normalized to the total protein content of the tissue lysate as determined by Bradford protein assay,[29] and is expressed in RLU/per mg protein.

Blood analysis. Blood samples were collected before euthanasia, and were sent to a commercial veterinary diagnostic laboratory (Phoenix Central Laboratory, Mukilteo, WA) for a complete blood count and a chemistry panel including ALT and AST, respectively, for detection of liver damage.[24]

Histological analysis. Treated and control liver biopsies were fixed in 10% neutral buffered formalin, then processed and embedded in paraffin. Routine hematoxylin and eosin and trichrome-stained slides were made to determine liver damage and evaluated by a clinical pathologist (K.R.L.).

REFERENCES

1. Miao, C and Brayman, AA (2011). Ultrasound-mediated gene delivery. In: Yuan, X (ed.). *Non-Viral Gene Therapy*. InTech: Rijeka, Croatia. pp. 213–242.
2. Mehier-Humbert, S and Guy, RH (2005). Physical methods for gene transfer: improving the kinetics of gene delivery into cells. *Adv Drug Deliv Rev* **57**: 733–753.
3. Liang, HD, Tang, J and Halliwell, M (2010). Sonoporation, drug delivery, and gene therapy. *Proc Inst Mech Eng H* **224**: 343–361.
4. Mayer, CR and Bekeredjian, R (2008). Ultrasonic gene and drug delivery to the cardiovascular system. *Adv Drug Deliv Rev* **60**: 1177–1192.
5. Stride, EP and Coussios, CC (2010). Cavitation and contrast: the use of bubbles in ultrasound imaging and therapy. *Proc Inst Mech Eng H* **224**: 171–191.
6. Suzuki, R, Oda, Y, Utoguchi, N and Maruyama, K (2011). Progress in the development of ultrasound-mediated gene delivery systems utilizing nano- and microbubbles. *J Control Release* **149**: 36–41.
7. Unger, EC, Matsunaga, TO, McCreery, T, Schumann, P, Sweitzer, R and Quigley, R (2002). Therapeutic applications of microbubbles. *Eur J Radiol* **42**: 160–168.
8. Chen, S, Ding, JH, Bekeredjian, R, Yang, BZ, Shohet, RV, Johnston, SA *et al.* (2006). Efficient gene delivery to pancreatic islets with ultrasonic microbubble destruction technology. *Proc Natl Acad Sci USA* **103**: 8469–8474.
9. Alter, J, Sennoga, CA, Lopes, DM, Eckersley, RJ and Wells, DJ (2009). Microbubble stability is a major determinant of the efficiency of ultrasound and microbubble mediated *in vivo* gene transfer. *Ultrasound Med Biol* **35**: 976–984.
10. Kodama, T, Aoi, A, Watanabe, Y, Horie, S, Kodama, M, Li, L *et al.* (2010). Evaluation of transfection efficiency in skeletal muscle using nano/microbubbles and ultrasound. *Ultrasound Med Biol* **36**: 1196–1205.
11. Laing, ST and McPherson, DD (2009). Cardiovascular therapeutic uses of targeted ultrasound contrast agents. *Cardiovasc Res* **83**: 626–635.
12. Porter, TR (2009). The utilization of ultrasound and microbubbles for therapy in acute coronary syndromes. *Cardiovasc Res* **83**: 636–642.
13. Shen, ZP, Brayman, AA, Chen, L and Miao, CH (2008). Ultrasound with microbubbles enhances gene expression of plasmid DNA in the liver via intraportal delivery. *Gene Ther* **15**: 1147–1155.
14. Song, S, Shen, Z, Chen, L, Brayman, AA and Miao, CH (2011). Explorations of high-intensity therapeutic ultrasound and microbubble-mediated gene delivery in mouse liver. *Gene Ther* **18**: 1006–1014.
15. Song, S, Noble, M, Sun, S, Chen, L, Brayman, AA and Miao, CH (2012). Efficient microbubble- and ultrasound-mediated plasmid DNA delivery into a specific rat liver lobe via a targeted injection and acoustic exposure using a novel ultrasound system. *Mol Pharm* **9**: 2187–2196.
16. Kamimura, K, Zhang, G and Liu, D (2010). Image-guided, intravascular hydrodynamic gene delivery to skeletal muscle in pigs. *Mol Ther* **18**: 93–100.
17. Duck, F (2009). Acoustic dose and acoustic dose-rate. *Ultrasound Med Biol* **35**: 1679–1685.
18. Miller, DL, Smith, NB, Bailey, MR, Czarnota, GJ, Hynynen, K and Makin, IR; Bioeffects Committee of the American Institute of Ultrasound in Medicine (2012). Overview of therapeutic ultrasound applications and safety considerations. *J Ultrasound Med* **31**: 623–634.
19. ter Haar, G (2010). Ultrasound bioeffects and safety. *Proc Inst Mech Eng H* **224**: 363–373.
20. Miller, DL and Dou, C (2009). Induction of apoptosis in sonoporation and ultrasonic gene transfer. *Ultrasound Med Biol* **35**: 144–154.
21. Vykhodtseva, N, McDannold, N and Hynynen, K (2006). Induction of apoptosis *in vivo* in the rabbit brain with focused ultrasound and Optison. *Ultrasound Med Biol* **32**: 1923–1929.
22. Dalecki, D (2004). Mechanical bioeffects of ultrasound. *Annu Rev Biomed Eng* **6**: 229–248.
23. Hwang, JH, Tu, J, Brayman, AA, Matula, TJ and Crum, LA (2006). Correlation between inertial cavitation dose and endothelial cell damage *in vivo*. *Ultrasound Med Biol* **32**: 1611–1619.
24. Green, RM and Flamm, S (2002). AGA technical review on the evaluation of liver chemistry tests. *Gastroenterology* **123**: 1367–1384.
25. Lee, YT (1978). Liver function tests after ligation of hepatic artery. *J Surg Oncol* **10**: 305–320.
26. Cullen, JM, Van den Ingh, TS, Bunch, SE, Rothuizen, J, Washabau, RJ and Desmet, VJ (2006). Morphological classification of circulatory disorders of the canine and feline livers. In: W.L.S. Group (ed.). *WSAVA Standards for Clinical and Histological Diagnosis of Canine and Feline Liver Disease*. Saunders Elsevier: Philadelphia, PA. pp. 41–59.
27. Kono, Y, Steinbach, GC, Peterson, T, Schmid-Schönbein, GW and Mattrey, RF (2002). Mechanism of parenchymal enhancement of the liver with a microbubble-based US contrast medium: an intravital microscopy study in rats. *Radiology* **224**: 253–257.
28. Rothuizen, J, Bunch, SE, Charles, JA, Cullen, JM, Desmet, VJ, Szatmari, V *et al.* (2006). *WSAVA Standards for Clinical and Histological Diagnosis of Canine and Feline Liver Disease*. Saunders Elsevier: Philadelphia, PA. pp. 130.
29. Bradford, MM (1976). A rapid and sensitive method for the quantitation of microgram quantities of protein utilizing the principle of protein-dye binding. *Anal Biochem* **72**: 248–254.